We are IntechOpen, the world's leading publisher of Open Access books Built by scientists, for scientists

4,800
Open access books available

122,000
International authors and editors

135M
Downloads

Our authors are among the

154
Countries delivered to

TOP 1%
most cited scientists

12.2%
Contributors from top 500 universities

CLARIVATE ANALYTICS BOOK CITATION INDEX INDEXED

WEB OF SCIENCE™

Selection of our books indexed in the Book Citation Index in Web of Science™ Core Collection (BKCI)

Interested in publishing with us?
Contact book.department@intechopen.com

Numbers displayed above are based on latest data collected.
For more information visit www.intechopen.com

19

Characterization of Melanoma Progression on Animal Model Using Fourier Transform Infrared Mapping

Beljebbar A.[1], Gatouillat G.[2], Morjani H.[1], Manfait M.[1] and Madoulet C.[2]
[1]*Unité MéDIAN, MEDyC CNRS UMR6237*
[2]*Laboratoire de Biochimie, IFR53 Biomolécules, UFR de Pharmacie, Université de Reims Champagne-Ardenne, 51 rue Cognacq-Jay, 51096 Reims Cedex, France*

1. Introduction

A majority of human cancers arise within the skin. The effective cure is surgical excision of the primary tumor (Thompson et al., 2005) when the lesions are smaller than 1 mm (James et al., 2000). Melanoma removal at early stages is almost always curative and therefore detection is essential. In fact, early detection of cancer is the most important factor in the prevention of cancer and a guarantee in most cases of an effective treatment or complete cure. Thus, the only reliable strategy to prevent death from melanoma still remains to be early diagnosis. The prognosis for a patient with stage I or II melanoma is mainly related to tumor thickness. Currently, the gold standard in most cancer diagnosis is histopathological evaluation, which involves the removal of tissue biopsies and examination by pathologists (Slater, 2000). This process includes tissue staining and morphological pattern recognition. During tissue transformation, it is expected that substantial modifications occur at molecular level before visible morphological changes become apparent. Hence, early detection is critical in melanoma treatment, and the evolution of the tumor and its penetration into the dermis are key factors to be studied in order to understand the disease (Elder, 2006). Melanoma is a tumor of melanocytes, which are a class of cells located at the epidermal-dermal junction. Observations in situ are limited, however, and tumor progression cannot be followed in humans due to ethical concerns.Therefore, appropriate animal model systems are needed. Second, the spatially-distributed nature of the tumor requires the use of imaging techniques but the influence of multiple cells requires biochemical contrast especially to study subtle molecular changes in early stage disease and its progression. The first is the development of model systems to study disease and the second is the development of new imaging technologies. Similarly, there have been efforts to characterize melanoma progression in biochemical terms, (Jeffs et al., 2009) including understanding the role of cells other than melanocytes in tumor evolution (Kempen et al., 2003). While characterization of tissue and tissue models is routinely accomplished by structural imaging, a biochemical characterization typically requires destruction of the structure, thereby losing spatially specific information. A combination of biochemical and structural knowledge is often helpful and is enabled by the emerging fields of chemical imaging and microscopy.

The main objective is a detection of the source of the pathological variation at molecular level in order to further understand the molecular carcinogenic process in a range of cancers. Indeed, tumor tissues are mostly heterogeneous in nature, and this heterogeneity further depends on the stage of disease and its aggressiveness. The emergence of a novel technique, complementary to histopathology and immunohistochemistry, can thus help in the early diagnostic of tissue transformation during carcinogenesis. Fourier-transform infrared microspectroscopy (FTIRM) has emerged as a powerful tool to study molecular structure and structural interactions in biological systems. When this technique is applied to tissues, the resulting spectra is composed of characteristic absorption bands originating from all infrared-active vibrational modes of biological macromolecules present in the tissue, such as proteins, lipids, and nucleic acids (Parker, 1971). Each of these molecules provides a unique absorption spectral pattern named fingerprint through the entire infrared spectrum. This property offers a way to identify the molecule type (qualitative analysis) and the amount or quantity of this molecule in the sample (quantitative analysis) (Beljebbar et al., 2008). This method can be used as a diagnostic tool, complementary to histopathology or immunochemistry (Fernandez et al., 2005). As the image contrast is based on the intrinsic vibrational signature of the tissue components, spectral images does not require the use of added dyes or labelling methods for visualization of different chemical components in the sample (Bates, 1976). Indeed, FT-IRM imaging combined a high spatially resolved morphological and biochemical information that offer a number of advantages for ex-vivo assessment of tissue and aid the histopathologist in the identification and classification of subtle biochemical changes related to carcinogenesis (Petibois & Déléris, 2006; Cohenford & Rigas, 1998). The use of a high spectral resolution and appropriate data treatment are of fundamental importance to isolate representative spectral markers of biocomponents. Correlations of morphologic and biochemical skin tissue differences could be used to identify variations that occur between healthy and diseased tissues. The development of clinical protocols for the routine examination of tissue histology or for localized tumors using IR microspectroscopic methods has been largely used in medical diagnostics of tumors (Wong et al, 1991; Rigas et al, 1990; Krafft, 2006, 2007; Amharref et al, 2006; Beljebbar et al., 2008). Previous studies have investigated the structure of skin (Garidel, 2002, 2003), diseases (Tfayli et al., 2005, Hammody et al., 2005, 2008; Ly et al., 2008) dynamics of diffusion (Mendelsohn et al., 2003, 2006; Morganti et al., 1999; Dary et al., 2001; Tetteh et al., 2009) or use it as a model system for studies (Bhargava and Levin., 2004). In vivo Raman and IR studies have not examined skin cancers, but focus on the effect of hydration and penetration enhancers on the stratum corneum (Pirot et al, 1997; Casper et al, 2003). Ex vivo IR studies indicate differences between skin tumors and normal skin (Wong et al, 1993); however, such studies have not taken into account the effect of the heterogeneous nature of the skin.

Infrared spectra contain many overlapping bands and so data interpretation cannot be made by simple visual inspection and alternative approaches are needed. Because of the high complexity of the FTIR spectra obtained from tissues, multivariate statistical methods are required to extract biochemical information related to tissue. This would permit to objectively differentiate distinct tissue structures and for identifying origin that gave rise to the specific tissue pathology. These methods have had a major impact on the quantitative and qualitative analysis of infrared spectral data. They have been shown to improve analysis precision, accuracy, reliability, and applicability for infrared spectral analyses relative to the more conventional univariate methods of data analysis. Rather than

attempting to find and use only an isolated spectral feature in the analysis of spectral data, multivariate methods derive their power from the simultaneous use of multiple intensities (i.e. multiple variables) in each spectrum (Mourant et al., 2003). During the last decade, it has been recognized that FT-IR, in combination with the appropriate multivariate analysis strategies, has considerable potential as a metabolic fingerprinting tool for the rapid detection and diagnosis of disease or dysfunction (Goodacre et al., 2004; Diem et al., 1999). Multivariate imaging techniques including Unsupervised Hierarchical Cluster Analysis (UHCA) (Jackson et al., 1998; Mohlenhoff et al., 2005), K-means clustering (Lasch et al., 2004; Zhang et al., 2003), Principal Components Analysis (PCA) (Lasch and Naumann, 1998), Linear Discriminant Analysis (LDA) (Mansfield et al, 1999), Fuzzy C-means clustering (Lasch et al., 2004; Mansfield et al., 1997) and neural networks (Lasch and Naumann, 1998) have proven to be invaluable in the identification of spectral groups or "clusters" which can be directly compared to stained tissue sections. In multivariate methods, the information of the entire spectrum can be utilized for the analysis. The high correlation of spectral clusters with anatomical and histopathological features has been conclusively demonstrated for a number of different tissue types.

Thus, the objective of this study will be to detect the source of the pathological variation at molecular level in order to further understand the molecular carcinogenic process in a range of melanoma disease, and the development of FTIRM to provide non-destructive, rapid, reproducible diagnosis, and minimize inter-observer variability. The identification and quantification of these specific molecular changes within skin can provide diagnostic information for aiding in early detection of diseases and their optimized treatment. The aim of this chapter will be the monitoring and interpretation of molecular changes associated to melanoma growth and invasion by FTIRM imaging on animal models.

2. FTIR characterization of normal skin tissues and melanoma progression using cluster analysis

2.1 Animals and cell lines

Six- to eight-week-old female B6D2F1 mice were purchased from the Charles River Laboratories (Iffa Credo, L'Arbresle, France) and housed at the animal maintenance facility of the Centre de Biotechnologies, U.F.R. Pharmacy, Reims, France. The treatments of mice protocols were according to the Institutional Animal Care and Use Committee guidelines.

B16R, a pigmented mouse melanoma cell line from C57Bl/6 (H-2b) origin resistant to 3.5 x 10^{-7} M doxorubicin was obtained from National Tumour Institute of Milan (Mariani et al., 1990). B16R were maintained in 5% CO_2 atmosphere at 37°C, in complete RPMI 1640 medium (Invitrogen, Cergy-Pontoise, France) supplemented with 10% heat-inactivated FBS (Invitrogen).

2.2 Tumour induction

For tumor induction, B6D2F1 mouse (five animals per group) were shaved on the right flank and subcutaneously challenged with 1 x 10^6 viable B16R cells in NaCl 0.9%. The size of the tumors was assessed in a blinded, coded fashion twice weekly and recorded as tumor area (in square cM) by measuring the largest perpendicular diameters with callipers. The experiment was repeated twice. The melanoma tumors were obtained by the injection of melanoma cell suspension in mice skin (Odot et al., 2004; Joseph-Pietras et al., 2006, 2007). B16R melanoma cells in B6D2F1 mice after subcutaneous injection is a well-established

model. This may prove to be a good model for investigation of local growth of tumor cells and their interaction with metastatic lesions. However, the histological progression from injected cells to establish local growth of melanoma has not been studied systematically. We therefore have investigated the molecular changes and growth of B16R melanoma at the injection site during eleven days post-implantation to identify spectroscopic markers associated to early detection of tissue transformation. One million B16F10 melanoma cells were injected subcutaneously in B6D2F1 mice. All animals' developed tumors with reproducible localization and size around the site of injection (Fig. 1).

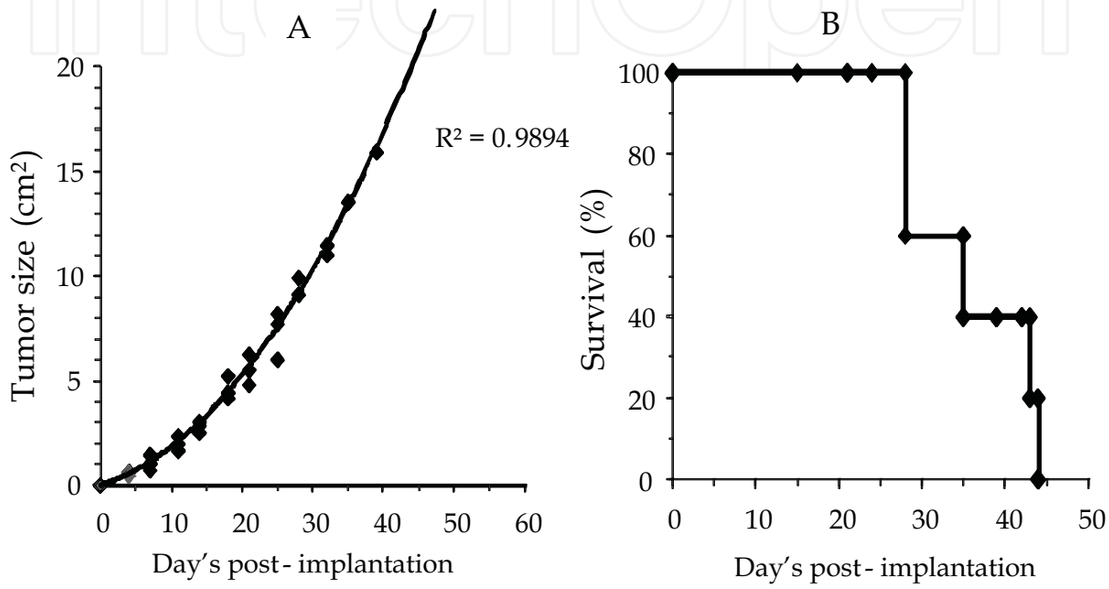

Fig. 1. Tumor development and survival of mice after subcutaneous injection of 1×10^6 B16R cells. Tumor size dependent on the period elapsed after injection of B16R cells. All animals with implanted B16R cells developed tumors with reproducible localization and size around the site of injection

These groups were sacrificed after 4, 7, 11 days post-implantation. After skin excision, tissue samples were snap-frozen by immersion in methyl-butane cooled down in liquid nitrogen and stored at - 80°C. Two adjacent sections were cut from each sample using a cryomicrotome. One section, 10 µm thick, was placed onto infrared transparent calcium fluoride (CaF_2) slides for infrared imaging. The second section, 7 µm thick, was placed on a microscope glass slide and stained with hematoxylin and eosin (H&E) for histopathological image.

2.3 Spectroscopic measurement

Spectra were collected using an FTIR imaging system (SPOTLIGHT, Perkin-Elmer, France) coupled to a FTIR spectrometer (Spectrum 300, Perkin-Elmer, France). This system is equipped with a liquid N_2 cooled Mercury-Cadmium-Telluride (MCT) line detector comprised of 16 pixel elements. The microscope was equipped with a movable, software-controlled x, y stage. In this study, FTIR images were collected from selected areas with a spatial resolution of 25 µm/pixel, in transmission mode, in the 4000–720 cm^{-1} range, with a final spectral resolution of 4 cm^{-1}, and 16 scans per pixel. After atmospheric correction, data

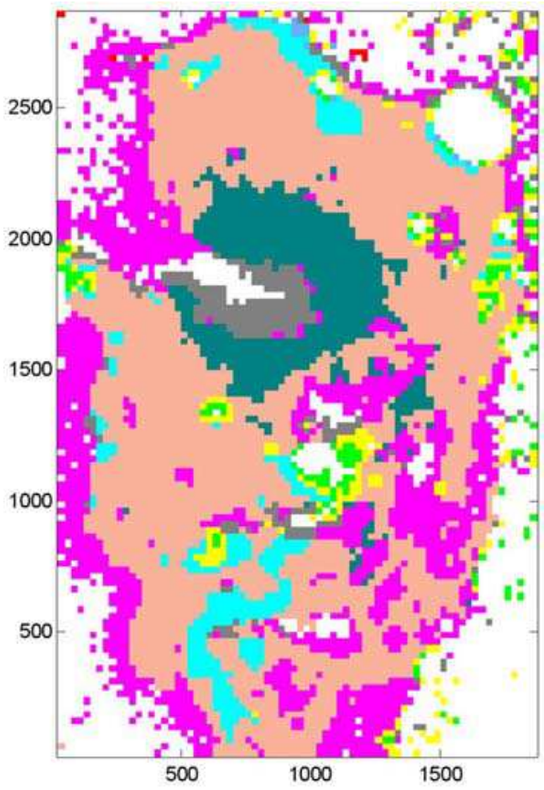

Day 4

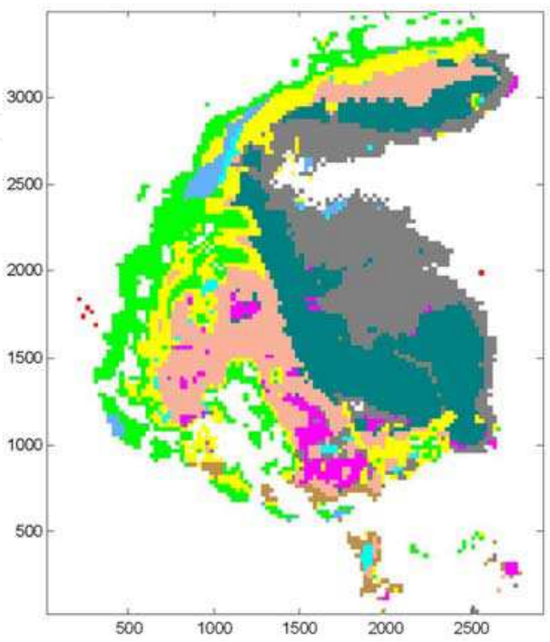

Day 7

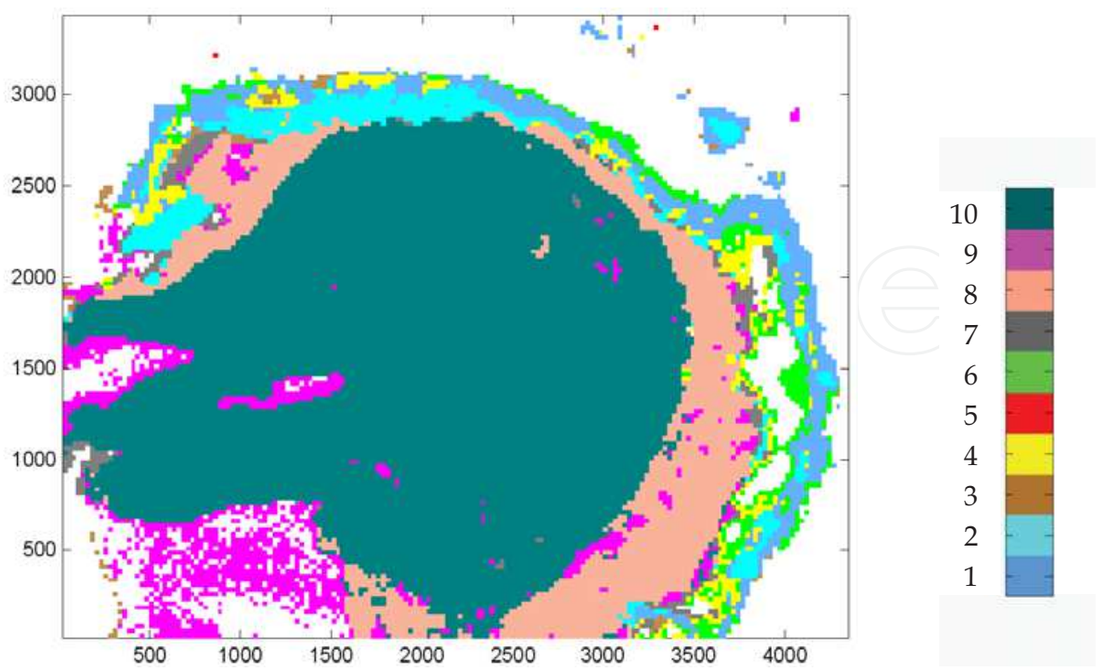

Day 11

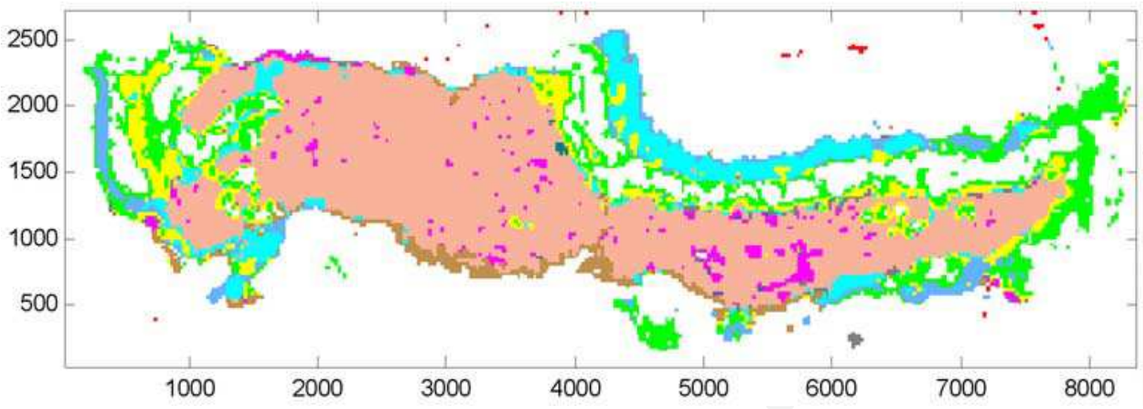

Fig. 2. All data measured on several skin tissues during tumor evolution were pooled in one dataset, processed at the same time to extract all features describing both normal and tumor tissues. Data were cut into the fingerprint region (900 to 1800 cm^{-1}) and cluster analysis was carried out on the first derivative spectra (to enhance the resolution of superimposed bands). K-means was calculated the cluster-membership of spectra by assigning each color to one class. Pseudo color FTIR maps on normal skin and tumor progression at 4, 7, 11 days post-implantation were constructed

were cut to fingerprint region (900 to 1800 cm^{-1}), converted to their first derivative, and smoothed using a seven point Savitzky-Golay algorithm in order to minimise the influence of background scatter in the spectra (Swieringa et al., 1999). The resulting spectra were then normalized using a Standard Normal Variate (SNV) procedure (Barnes and Dhanoa, 1989). A multivariate statistical analysis (Principal Component Analysis (PCA) and K-Means (KM)) was performed on this dataset. K-means clustering was performed on these principal component scores. Pseudo-color maps based on cluster analysis were then constructed by assigning a color to each spectral cluster. The cluster spectra were calculated by averaging absorbance spectra associated to each group and used for the interpretation of the chemical or biochemical differences between clusters. All data measured on normal skin and melanoma development (from 4 to 11 days growth) were pooled in one dataset, processed at the same time and the results were displayed as pseudo-color maps with the same color scale. In this way, we can easily determine all their common and discriminating features by comparing their infrared maps.

2.4 Discrimination between normal and melanoma progression

FTIR technique was used to identify biochemical changes associated to melanoma progression and invasion such as proteins, nucleic acid and lipids. Fig. 2 displays FTIR pseudo-color maps of skin tissues. 10 clusters describing both normal skin and cancer features were extracted and pseudo FTIR maps were constructed with the same color scale. Different clusters in the FTIR images were correlated to normal features. White color represents the area where no tissue was present. In the pseudo-color map obtained from normal skin, clusters 1 to 4 and 8 have described all normal structures. Cluster 8 encoded almost all normal skin and the other groups were associated to superficial skin layers. At day 4 post-implantation, two particular structures (clusters 7 and 10) were located in the melanoma cells injection site. These features were associated to B16 cell growth.

From day 7, the tumor is fairly large and deeply situated within the skin with massive infiltration into the tissue. Most of normal skin was destroyed by tumor tissue. Cluster 7 observed in the border of the tumor increased from 4 to 7 days post-implantation. This cluster disappeared and all tumor was described by cluster 10.

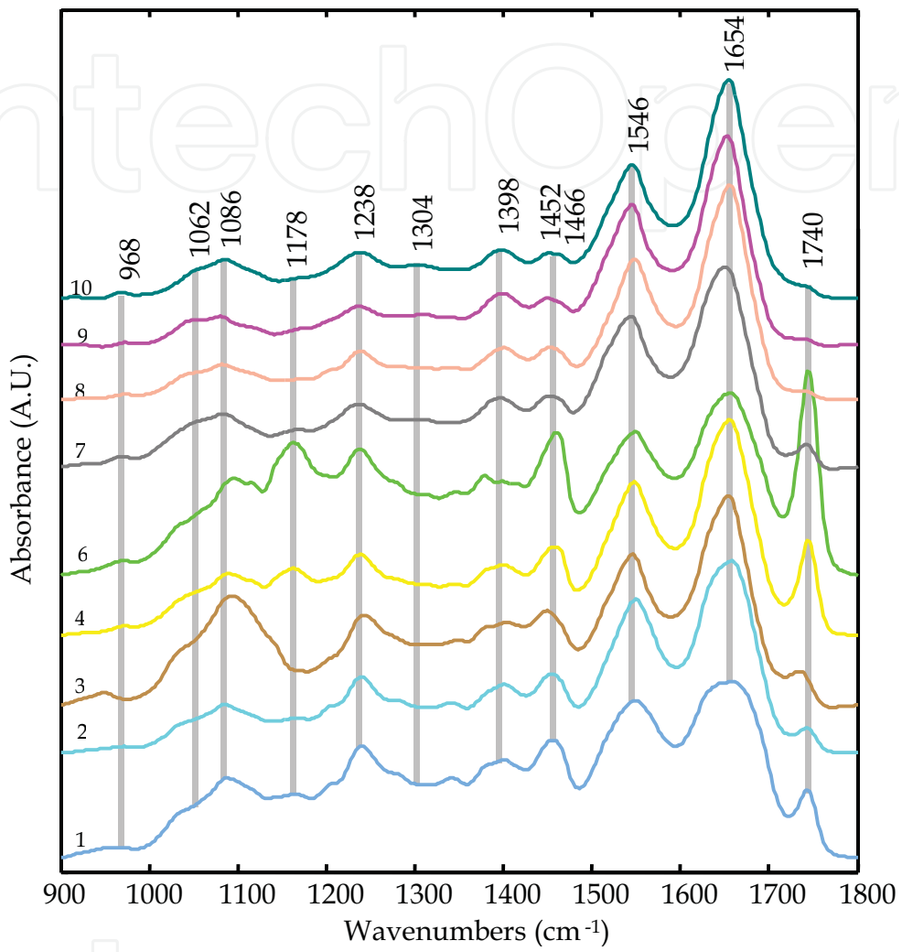

Fig. 3. Representative cluster mean FTIR spectra extracted from pseudocolor maps. Cluster averaged spectra were obtained by meaning absorbance spectra associated to each group. 10 models describing normal and melanoma skin development. Each cluster averaged spectrum assigned to one class was plotted with the same color than in pseudo-color map

Fig. 3 shows class average spectra of the normal skin and melanoma tumor tissues. These spectra are dominated by two absorbance bands at 1654 and 1546 cm^{-1} known as the amide I and II, respectively. The band at 1740 cm^{-1} arises from the stretching mode of C=O groups of lipids. The absorption band at 1398 is attributed to COO^- symmetric stretching vibrations of fatty acids and amino acids. The bands at 1238 cm^{-1} and 1086 cm^{-1} are due to the antisymmetric and symmetric phosphate stretching mode PO_2^{2-} of nucleic acids and phospholipids respectively. The relatively weak band at 1178 cm^{-1}, in the normal tissue is due to stretching mode of C–O groups of proteins. The band at 968 cm^{-1} is attributed to the dianionic PO_2^{2-} monoester of nucleic acids (DNA) and phospholipids. The bands at 1466

cm^{-1} and 1452 cm^{-1} were attributed respectively to CH_2 scissoring and antisymmetric deformation of CH_3 group. In normal skin, the intensity of antisymmetric deformation of CH_3 group (1452 cm^{-1}) is much greater than the intensity of the band at 1398 cm^{-1} attributed to COO^- symmetric stretching. However, in melanoma tumor, these two bands exhibit a similar intensity (clusters 7, 9, 10). Indeed, the band associated to C=O (1740 cm^{-1}) decreased from normal to melanoma tissues. Therefore in normal tissues, absorption from CH_2 groups of the lipid acyl chains dominates the band at 1466 cm^{-1}. In melanoma, these two bands arise predominantly from protein side chains. In a typical protein, side chains contain approximately equal proportions of CH_2 and CH_3 groups. The comparison between normal tissue and tumor counterpart shows a decreased and even disappearance of the bands at 1466 cm^{-1} and 1740 cm^{-1} associated to lipids and phospholipids in the melanoma tissues. Indeed, malignant tissues displayed the appearance of the band at 1062 cm^{-1} attributed to the C–C stretching and a decrease in the intensity of the band at 1082 due to phospholipids diminution compared to normal tissues. The variations in the spectral characteristics between the normal and malignant tissues provided a basis for clinical application.

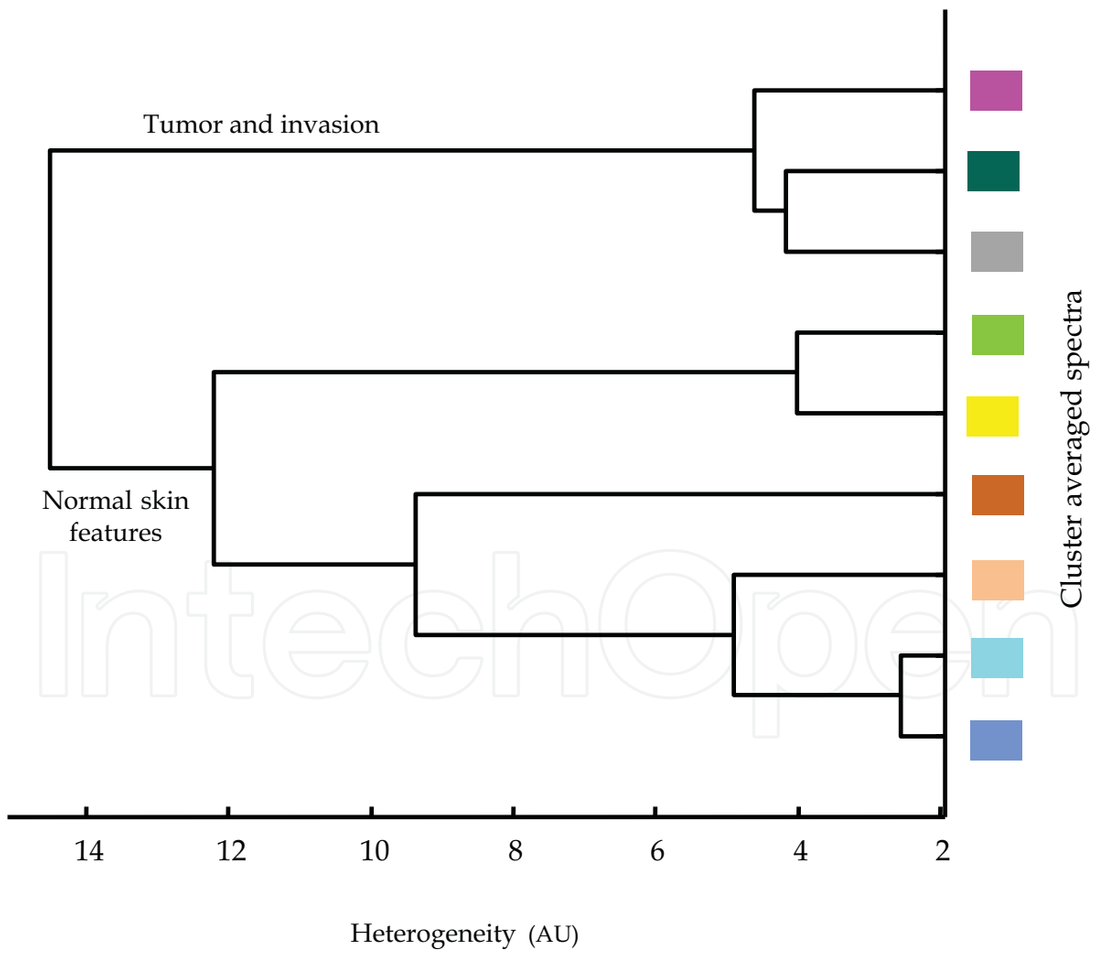

Fig. 4. Dendrogram obtained from hierarchical cluster analysis on spectral cluster averages associated to different tissue types. Heterogeneity represents the discriminating distance given by arbitrary units (AU)

We have used a cluster analysis to discriminate between normal and melanoma tissues. In fact, FTIR spectroscopy provides information on broad classes of molecules such as lipids, proteins, carbohydrates and make up the complex medium of cell and tissues. The spectrum from cells and tissues is an integration of these individual signals from all biomolecules (Diem et al., 2004). Since each molecular species is associated with specific frequencies, it may thus be possible to identify and quantify these biomolecules individually within the spectrum. Several authors have quantified individual constituents after tissue alteration. The models developed were used to explain the features present in the tissue/cellular spectra by using spectral data of pure molecules. The quantification of several biomolecules seen during tissue transformation can be used to classify disease states with high sensitivity, specificity, and accuracy. Wang et al. have investigated formalin-fixed Barrett's esophagus for predicting the underlying histopathology, the early detection and rapid staging of many diseases (Wang et al., 2007). Their model seems to be very accurate in spite of the presence of a number of common spectral features or molecular interactions and variations that can broaden individual peaks. Krafft *et al*. have developed a supervised classification model based on the LDA algorithm to IR images of three specimens from one patient (Krafft et al., 2007). There multivariate methods were used to develop a chemical/morphological model to quantify chemical composition of coronary atherosclerosis (Römer et al., 1998), breast tissue (Haka et al., 2005), porcine brain (Koljenovic et al., 2007), and molecular concentration profiles in the skin (Caspers et al., 2001).

To distinguish between normal and melanoma tissue, cluster averaged spectra obtained from pseudo-color maps were input in the hierarchical cluster analysis using Ward's clustering algorithm and the square Euclidian distance measure. Fig. 4 displayed the dendrogram associated to this classification. The result showed a clear distinction between all normal and tumor structures. Indeed, the class related to normal skin structures was divided to two sub-clusters associated to high lipid content (external layers) and low lipid constituents (internal layers).

3. Distribution of molecular changes in skin constituents associated to melanoma tumor

Peak ratios are commonly used to discriminate normal from tumor tissues. Krafft *et al*. have evaluated the usefulness of the lipid-to-protein ratio (2850/1655 cm^{-1}) as a spectroscopic marker to discriminate between normal and tumor tissue, as well as between low- and high-grade glioma tissues (krafft et al., 2007). We have investigated the spatial distribution of molecular changes between normal and melanoma. Integrated intensity bands ratio between the region 1360-1430 cm^{-1} and 1430-1480 cm^{-1}, attributed to COO^- symmetric stretching vibrations of fatty acids and amino acids and to CH_2 scissoring and antisymmetric deformation of CH_3 group respectively were calculated. Pseudo color maps scores were constructed (Fig. 5) in order to characterize the differences between healthy and pathological skin. The comparison between these pseudo color scores maps shows that high scores described the melanoma structure (colorbar). These scores decreased in the normal skin tissue. This intensity ratio was correlated to the changes in lipid content.

In our previous study, intensity ratios the 1466/1396cm^{-1} (amino acid side chain from peptides and proteins at 1466 and 1396 cm^{-1} were used to discriminate between normal and glioma brain tissue). Krafft et al. have demonstrated that this ratio is maximal for normal

brain tissue and decreases with the progression of the disease (Krafft et al., 2007). Another study reported a significant differences between the spectra of malignant breast cancers and benign breast tissues in the relative intensity ratios of different peaks (I1640/ I1550 and I1160/I1120 for protein structures; I1640/I1460 and I1550/I1460 for relative content of protein and lipid; I1460/I1400 for lipid structures; I1310/I1240 for nucleic acid).

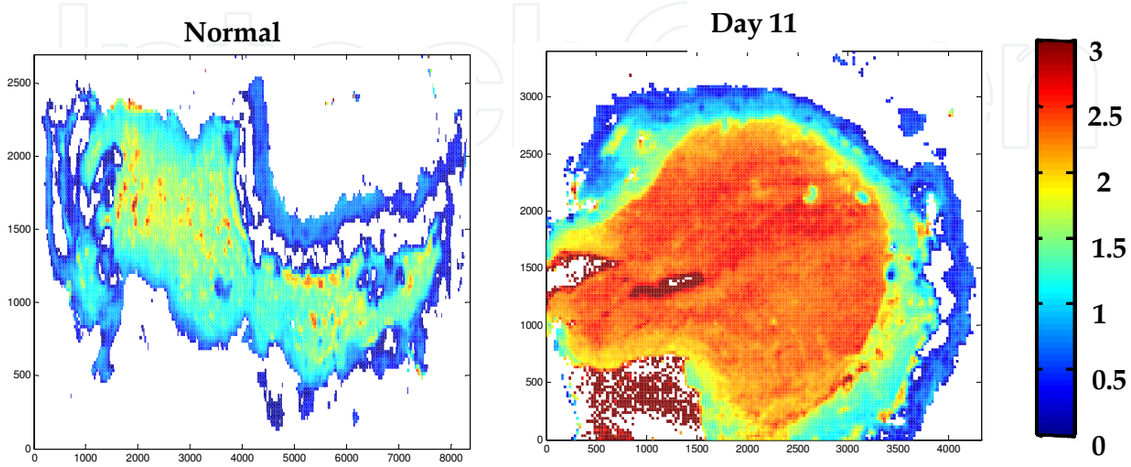

Fig. 5. Biochemical distribution of the changes in the molecular composition of tissues between normal and melanoma tumor at 11 days post-implantation. Maps of absorbance intensity ratios of bands in the region 1360-1430 and 1430-1480 were constructed and used to identify which biochemical markers could be more potential indicators of such variations between normal and melanoma tumor

4. Conclusion

In this study, we have demonstrated the potential of FTIR imaging combined to multivariate statistical analysis as rapid and objective tool to monitor the molecular histopathology alteration of skin tissue during melanoma growth without tissue staining. The identification and quantification of these specific molecular changes within skin can provide diagnostic information for aiding in early detection of diseases and their optimized treatment. We have monitored the molecular changes associated with melanoma growth and invasion by FTIRM imaging to better understand the tissue transformation during carcinogenesis.This study demonstrated that FT-IRM imaging, with high spatially resolved morphological and biochemical information can be used as a diagnostic tool to understand the tissue alteration. Multivariate statistical analysis such as cluster analysis allowed investigation of B16 melanoma progression (from day 4 to day 11 post implantation). Different clusters in the FTIR images were correlated to morphological and histological features. Our results showed that at 4 days after tumor implantation, FTIR investigations displayed a very small abnormal zone associated with the proliferation of B16 cells in the injection site. From this day, mice developed solid and well-circumscribed tumors. By using imaging technique, we were able to take in account the variance due to the heterogeneity of skin tissues. These constituents can be used as spectroscopic markers for early detection of tissue abnormality and discrimination among normal, invasion, and tumor.

5. References

Amharref, N., Beljebbar, A., Dukic, S., Venteo, L., Schneider, L., Pluot, M., Vistelle, R.. & Manfait, M. (2006). Brain tissue characterisation by infrared imaging in a rat glioma model. *Biochim. Biophys. Acta*, Vol. 1758, No. 7, (07.2006) 892-899, ISSN 00052736

Barnes, R.J., Dhanoa, M.S. & Lister, S.J. (1989). Standard normal variate transformation and de-trending of near-infrared diffuse reflectance spectra. *Appl. Spectrosc.*, Vol. 43, No. 5, (07.1989), pp. 772-777, ISSN 00037028

Bates, J.B. (1976). Fourier transform infrared spectroscopy. *Science, Vol.* 9, No. 191, 4222, (01.1976), pp. 31-37, ISSN 00368075

Beljebbar, A., Amharref, N., Lévèques, A., Dukic, S., Venteo, L., Schneider, L., Pluot, M., & Manfait, M. (2008). Modeling and quantifying biochemical changes in C6 tumor gliomas by Fourier transform infrared imaging. *Anal. Chem.*, Vol. 15, No 80, (11.2008), pp. 8406-8415, ISSN 00032700

Beljebbar, A., Amharref, N., Lévèques, A., Dukic, S., Venteo, L., Schneider, L., Pluot, M., & Manfait M. (2008). Modeling and quantifying biochemical changes in C6 tumor gliomas by Fourier transform infrared imaging. *Anal. Chem, Vol.*80, No22, (11.2008), pp. 8406-8415, ISSN 1520-6882

Bhargava, R. & Levin, I.W. (2004). Gram-Schmidt orthogonalization for rapid reconstructions of Fourier transform infrared spectroscopic imaging data. *Appl. Spectrosc.*, Vol. 58, No. 8, (08.2004), pp. 995–1000, ISSN 0003-7028

Caspers, P.J., Lucassen, G.W., & Puppels, G.J. (2003). Combined in vivo confocal Raman spectroscopy and confocal microscopy of human skin. *Biophys. J.*, Vol. 85, No. 1, (07.2003), pp.52–61, ISSN 0006-3495

Caspers, P.J., Lucassen, G.W., Carter, E.A., Bruining, H.A. & Puppels, G.J. (2001). In vivo confocal Raman microspectroscopy of the skin: noninvasive determination of molecular concentration profiles. *J. Invest. Dermatol.*, Vol. 116, No. 3, (03.2001), pp. 434-442, ISSN 0022-202X

Cohenford, M.A. & Rigas B. (1998). Cytologically normal cells from neoplastic cervical samples display extensive structural abnormalities on IR spectroscopy: implications for tumor biology. *Proc. Natl. Acad. Sci. U S A.*, Vol. 95, No. 26, (12.1998), pp. 15327–15332, ISSN 00278424

Dary, C.C., Blancato J.N. & Saleh, M.A. (2001). Chemomorphic analysis of malathion in skin layers of the rat: implications for the use of dermatopharmacokinetic tape stripping in exposure assessment to pesticides. *Regul. Toxicol. Pharmacol.*, Vol. 34, No. 3, (12.2001), pp. 234–248, ISSN 0273-2300

Diem, M., Boydston-White, S. & Chiriboga, L. (1999). Infrared spectroscopy of cells and tissues: shining light onto a novel subject. *Appl. Spectrosc.*, Vol. 53, No. 4, pp. 148-161, ISSN 00037028

Diem, M., Romeo, M., Boydston-White, S., Miljković, M. & Matthäus, C. (2004). A decade of vibrational micro-spectroscopy of human cells and tissue (1994-2004).*Analyst*, Vol. 129, No. 10, (10.2004), pp. 880–885, ISSN 0003-2654

Elder, D.E. (2006). Pathology of melanoma. *Clin. Cancer Res.*, Vol. 12, No. 7 Pt 2, (01.2006), pp. 2308s–2311s, ISSN 1078-0432

Fernandez, D.C., Bhargava, R., Hewitt, S.M.& Levin, I.W. (2005). Infrared spectroscopic imaging for histopathologic recognition. *Nature Biotechnology,* Vol. 23, No. 4, pp. 469-474, ISSN 10870156

Garidel, P. (2002). Mid-FTIR-Microspectroscopy of stratum corneum single cells and stratum corneum tissue *Phys. Chem. Chem. Phys*., Vol. 4, No. 22, pp. 5671–5677, ISSN 1463-9076

Goodacre, R., Vaidyanathan, S., Dunn, W.B., Harrigan, G.G. & Kell, D.B. (2004). Metabolomics by numbers: Acquiring and understanding global metabolite data, *Trends Biotechnol.*, Vol. 22, No. 5, (05.2004), pp. 245–252, ISSN 01677799

Haka, A.S., Shafer-Peltier, K.E., Fitzmaurice, M., Crowe, J., Dasari, R.R. &Feld, M.S. (2005). Diagnosing breast cancer by using Raman spectroscopy. *Proc. Natl. Acad. Sci. USA*, Vol. 102, No. 35, (08.2005), pp. 12371–12376, ISSN 0027-8424

Hammody, Z., Agrov, S., Sahu, R.K., Cagnano, E., Moreh, R. & Mordechai, S. (2008). Distinction of malignant melanoma and epidermis using IR micro-spectroscopy and statistical methods. *Analyst*, Vol. 133, No. 3, (03.2008), pp. 372–378, ISSN 0003-2654

Hammody, Z., Sahu, R.K., Mordechai, S., Cagnano E. & Argov, S. (2005). Characterization of malignant melanoma using vibrational spectroscopy. *Sci. World J.*, Vol. 5, No. 5, (03.2005), pp.173–182, ISSN 1537-744X

Jackson, M., Ramjiawan, B., Hewko, M., & Mantsch, H.H.. (1998). Infrared microscopic functional group mapping and spectral clustering analysis of hypercholesteramic rabbit liver. *Cell. Mol. Biol*., Vol. 44, No. 1, (02.1998), pp. 89–98, ISSN 01455680

James, W.D., Berger ,T.G. & D. Elston, Andrews' Diseases of the Skin, 9th ed. 2000, Philadelphia, pp. 881–889

Jeffs, A. R. , Glover, A. C., Slobbe, L. J., Wang, L. , He, S.J., Hazlett, J.A., Awasthi, A., Woolley, A.G., Marshall, E.S., Joseph W.R., Print C.G., Baguley B.C. & Eccles M.R., (2009) A gene expression signature of invasive potential in metastatic melanoma cells.PLoS One, Vol., No12, (12.2009), pp. e8461, ISSN 1932-6203

Joseph-Pietras, D., Carlier, A., Madoulet, C. & Albert, Ph. (2007). Cytostatic murine B16 cell pulsed Dendritic Cells induce effective protection against melanoma in mice. *Anticancer Res*., Vol. 27, No. 6B, (11.2007), pp. 3863-3872, ISSN 0250-7005

Joseph-Pietras, D., Carlier, A., Madoulet, C. and Albert, Ph. (2006). Anti-tumoral activity of peripheral blood mononuclear cells against melanoma cells: discrepant *in vitro* and *in vivo* effects. *Melanoma Res.*, Vol. 16, No. 4, (08.2006), pp. 325-33, ISSN 0960-8931

Koljenovic, S. Bakker Schut, T.C.,Wolthuis, R.,Vincent, A.J., Hendriks-Hagevi, G., Santos, L., Kros, J.M.& Puppels, G.J. (2007). Raman spectroscopic characterization of porcine brain tissue using a single fiber-optic probe. *Anal. Chem*., Vol. 79, No. 2, (01.2007), pp. 557-564, ISSN 0003-2700

Krafft, C. & Sergo V. (2006). Biomedical applications of Raman and infrared spectroscopy to diagnose tissue. *Spectrosc. Int. J.*, Vol. 20, No. 5, (01.2006), pp. 195–218, ISSN 0712-4813

Krafft, C., Neudert, L., Simat, T., & Salzer, R. (2005). Near infrared Raman spectra of human brain lipids. *Spectrochim. Acta (Part A),* Vol. 61, No. 7, (05 2005), pp. 1529-1535, ISSN 13861425

Krafft, C., Sobottka, S.B., Geiger, K.D., Schackert, G., & Salzer, R. (2007). Classification of malignant gliomas by infrared spectroscopic imaging and linear discriminant analysis. *Anal. Bioanal. Chem.*, Vol. 387, No. 5, (03 2007), pp. 1669-1677, ISSN 16182642

Krafft, C., Sobottka, S.B., Schackert, G., & Salzer R. (2006). Raman and infrared spectroscopic mapping of human primary intracranial tumors: A comparative study. *J. Raman Spectrosc.*, Vol. 37, No. 1-3, (01 2006), pp. 367-375, ISSN 03770486

Lasch, P & Naumann D. (1998). FT-IR microspectroscopic imaging of human carcinoma thin sections based on pattern recognition techniques. *Cell. Mol. Biol.*, Vol. 44, No. 1, (02.1998), pp. 189–202, ISSN 01455680

Lasch, P., Haensch, W., Naumann, D., & Diem, M. (2004). Imaging of colorectal adenocarcinoma using FT-IR microspectroscopy and cluster analysis. *Biochim Biophys Acta., Vol.* 1688, No. 2, (03.2004), pp. 176–186, ISSN 09254439

Ly, E., Piot, O., Wolthuis, R., Durlach, A., Bernard, P. & Manfait, M. (2008). Combination of FTIR spectral imaging and chemometrics for tumour detection from paraffin-embedded biopsies. *Analyst*, Vol. 133, No. 2, (02.2008), pp. 197–205, ISSN 0003-2654

Mendelsohn, R., Chen, H.C., Rerek, M.E. & Moore, D. J. (2003). Infrared microspectroscopic imaging maps the spatial distribution of exogenous molecules in skin. *J. Biomed. Opt.*, Vol. 8, No. 2, (04.2003), pp. 185–190, ISSN 1083-3668

Mendelsohn, R., Flach, C.R. & Moore, D.J. (2006). Determination of molecular conformation and permeation in skin via IR spectroscopy, microscopy, and imaging. *Biochim. Biophys. Acta, Biomembr.*, Vol. 1758, No. 7, (07.2006), pp. 923–933, ISSN 0006-3002

Mohlenhoff, B., Romeo, M., Diem, M., & Wood, B.R. (2005). Mie-type scattering and non-Beer-Lambert absorption behaviour of human cells in infrared microspectroscopy. *Biophys J., Vol.* 88, No. 5, (05.2005), pp. 3635–3640, ISSN 00063495

Morganti, F., Bramanti, E., Solaro, R., Benedetti, E., Chiellini, E., Nannipieri, E., Narducci, P., Krauser, S.F. & Samour, C.M. (1999) Thermal and spectroscopic characterization of interactions between 2-nonyl-1,3-dioxolane and stratum corneum components. *J. Bioact. Compat. Polym.*, Vol. 14, No. 2, (03.1999), pp. 162–177, ISSN 08839115

Mourant, J.R., Yamada, Y.R. Carpenter, S., Dominique, L.R. & Freyer, J.P. (2003). FTIR spectroscopy demonstrates biochemical differences in mammalian cell cultures at different growth stages. *Biophys. J.*, Vol. 85, No. 3, (09.2003) 1938–1947, ISSN 00063495

Odot, J., Albert, Ph., Carlier, A., Tarpin, M., Devy, J. & Madoulet C. (2004). *In vitro* and *in vivo* anti-tumoral effect of curcumin against melanoma cells. *Int. J. Cancer*, Vol. 111, No. 3, (09.2004), pp. 381-387, ISSN 0020-7136

Parker, F. S., (1971*). Application of infrared spectroscopy in biochemistry, biology and medicine* Plenum, New York

Petibois, C. & Déléris, G. (2006). Chemical mapping of tumor progression by FT-IR imaging: towards molecular histopathology. *Trends in Biotechnology*, Vol. 24, No. 10, (08.2006), pp. 455-462, ISSN 01677799

Pirot, F., Kalia, Y.N., Stinchcomb, A.L., Keating, G., Bunge, A. & Guy, R.H. (1997). Characterization of the permeability barrier of human skin in vivo. *Proc. Natl. Acad. Sci US, Vol.* 94, No. 4, (02.1997), pp.1562–1567, ISSN 0027-8424

Rigas, B., Morgello, S., Goldman, I., & Wong, P. (1990). Human colorectal cancers display abnormal Fourier-transform infrared spectra. *Proc. Natl. Acad. Sci. USA*, Vol. 87, No. 20, (10.1990), pp. 8140–8144, ISSN 00278424

Römer, T.J., Brennan, J.F., Fitzmaurice, M., Feldstein, M.L., Deinum, G., Myles, J.L., Kramer, J.R., Lees, R.S., Feld, M.S. (1998). Histopathology of human coronary atherosclerosis by quantifying its chemical composition with Raman spectroscopy. *Circulation*, Vol. 10, No. 9, (03.1998), pp. 878-885, ISSN 0009-7322

Savitzky, A. & Golay, M.J.E. (1964). Smoothing and differentiation of data by simplified least squares procedures. Anal. *Chem.*, Vol. 36, No. 8, (08 1964), pp. 1627-1639, ISSN 0003-2700

Slater, D.N. (2000). Doubt and uncertainty in the diagnosis of melanoma. *Histopathology*, Vol. 37, No. 5, (11.2000), pp. 469–472, ISSN 1365-2559

Swieringa, H., de Weijer A.P., van Wijk, R.J.& Buydens, L.M.C. (1999). Strategy for Constructing Robust Multivariate Calibration Models. *Chemometrics and Intelligent laboratory systems*, Vol. 49, No. 1, pp. 1-28, ISSN 0169-7439

Tetteh, J., Mader, K.T., Andanson, J.M., McAuley, W.J., Lane, M.E., Hadgraft, J., Kazarian, S.G. & Mitchell, J.C. (2009). Local examination of skin diffusion using FTIR spectroscopic imaging and multivariate target factor analysis. *Anal. Chim. Acta*, Vol. 642, No. 1-2, (05.2009), pp. 246–256, ISSN 1873-4324

Tfayli, A., Piot, O., Durlach, A., Bernard, P. & Manfait, M. (2005). Discriminating nevus and melanoma on paraffin-embedded skin biopsies using FTIR microspectroscopy. *Biochim. Biophys. Acta, Gen. Subj.*, Vol. 1724, No. 3, (08.2005), pp. 262–269, ISSN 0006-3002

Thompson, J.F., Scolyer, R.A. & Kefford, R .F. (2005). Cutaneous melanoma, *Lancet*, Vol., 365, No. 9460, (02.2005), pp. 687–701, ISSN 1474-547X

van Kempen, L.C., Ruiter, D., van Muijen, G.N. & Coussens, L.M. (2003). The tumor microenvironment: a critical determinant of neoplastic evolution. *Eur. J. Cell Biol.*, Vol. 82, No. 11, (11.2003), pp. 539–548, ISSN 0171-9335

Wang, T.D., Triadafilopoulos, G., Crawford, J.M.,, Dixon, L.R., Bhandari, T., Sahbaie, P., Friedland, S., Soetikno, R., and Contag, C.H. (2007) Detection of endogenous biomolecules in Barrett's esophagus by Fourier transform infrared spectroscopy. *Proc. Natl. Acad. Sci. USA*, Vol. 104, No. 40, (10.2007), pp. 15864–15869, ISSN 0027-8424

Wong, P.T., Wong, R.K., Caputo, T.A., Godwin, T.A. & Rigas, B. (1991). Infrared spectroscopy of exfoliated human cervical cells: Evidence of extensive structural changes during carcinogenesis. *Proc. Natl. Acad. Sci. USA*, Vol. 88, No. 24, (12.1991), pp. 10988–10992, ISSN 00278424

Wong, P.T.T., Goldstein, S.M., Grekin, R.C., Godwin, T.A., Pivik, C. & Rigas, B. (1993). Distinct infrared spectroscopic patterns of human basal cell carcinoma of the skin. Cancer Res., Vol. 53, No. 4, (02.1993), pp. 762–765, ISSN 0008-5472

Zhang, G.J., Moore, D.J., Flach, C. R. & Mendelsohn, R. (2007). Vibrational microscopy and imaging of skin: from single cells to intact tissue. *Anal. Bioanal. Chem.*, Vol. 387, No. 5, (03.2007), pp. 1591–1599, ISSN 1618-2642

Zhang, L., Small, G.W., Haka, A.S., Kidder, L.H., & Lewis, E.N. (2003). Classification of Fourier transform infrared microspectroscopic imaging data of human breast cells by cluster analysis and artificial neural networks. *Appl. Spectrosc.*, Vol. 57, No. 1, (01.2003), pp. 14–22, ISSN 00037028

Zhou, S., Xu, Z., Ling, X.F., Li, Q.B., Xu, Y.Z., Zhang, L., Zhao, H.M., Wang, L.X., Hou, K.Y., Zhou, X.S. & Wu JG. (2006). FTIR spectroscopic characterization of freshly removed breast cancer tissues. *Zhonghua Zhong Liu Za Zhi.*,Vol. 28, No. 7, (07.2006), pp. 512-514, ISSN 0253-3766

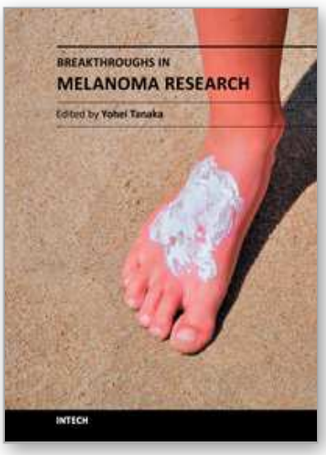

Breakthroughs in Melanoma Research

Edited by Dr Yohei Tanaka

ISBN 978-953-307-291-3
Hard cover, 628 pages
Publisher InTech
Published online 30, June, 2011
Published in print edition June, 2011

Melanoma is considered to be one of the most aggressive forms of skin neoplasms. Despite aggressive researches towards finding treatments, no effective therapy exists to inhibit the metastatic spread of malignant melanoma. The 5-year survival rate of metastatic melanoma is still significantly low, and there has been an earnest need to develop more effective therapies with greater anti-melanoma activity. Through the accomplishment of over 100 distinguished and respected researchers from 19 different countries, this book covers a wide range of aspects from various standpoints and issues related to melanoma. These include the biology of melanoma, pigmentations, pathways, receptors and diagnosis, and the latest treatments and therapies to make potential new therapies. Not only will this be beneficial for readers, but it will also contribute to scientists making further breakthroughs in melanoma research.

InTech Europe
University Campus STeP Ri
Slavka Krautzeka 83/A
51000 Rijeka, Croatia
Phone: +385 (51) 770 447
Fax: +385 (51) 686 166
www.intechopen.com

InTech China
Unit 405, Office Block, Hotel Equatorial Shanghai
No.65, Yan An Road (West), Shanghai, 200040, China
中国上海市延安西路65号上海国际贵都大饭店办公楼405单元
Phone: +86-21-62489820
Fax: +86-21-62489821

IntechOpen